Title

Structural Dynamics of Agonist and Antagonist Binding to the Androgen Receptor

Journal

The Journal of Physical Chemistry B, 123(36)

ISSN

1520-6106

Authors

Singam, Ettayapuram Ramaprasad Azhagiya
Tachachartvanich, Phum
La Merrill, Michele A
et al.

Publication Date

2019-09-12

DOI

10.1021/acs.jpcb.9b05654

Peer reviewed

HHS Public Access

Author manuscript

J Phys Chem B. Author manuscript; available in PMC 2019 September 12.

Published in final edited form as:

J Phys Chem B. 2019 September 12; 123(36): 7657–7666. doi:10.1021/acs.jpcb.9b05654.

Structural Dynamics of Agonist and Antagonist Binding to the Androgen Receptor

Ettayapuram Ramaprasad Azhagiya Singam[1], **Phum Tachachartvanich**[2], **Michele A. La Merrill**[2], **Martyn T. Smith**[3,*], **Kathleen A. Durkin**[1,*]

[1]Molecular Graphics and Computation Facility, College of Chemistry, University of California, Berkeley, CA, USA

[2]Department of Environmental Toxicology, University of California, Davis, CA, USA

[3]Division of Environmental Health Sciences, School of Public Health, University of California, Berkeley, CA, USA

Abstract

Androgen receptor (AR) is a steroid hormone nuclear receptor which upon binding its endogenous androgenic ligands (agonists), testosterone and dihydrotestosterone (DHT), alters gene transcription producing a diverse range of biological effects. Anti-androgens, such as the pharmaceuticals bicalutamide and hydroxyflutamide, act as agonists in the absence of androgens and as antagonists in their presence or in high concentration. The atomic level mechanism of action by agonists and antagonists of AR is less well characterized. Therefore, in this study, multiple 1 μs molecular dynamics (MD), docking simulations and perturbation-response analyses were performed to more fully explore the nature of interaction between agonist or antagonist and AR and the conformational changes induced in the AR upon interaction with different ligands. We characterized the mechanism of the ligand entry/exit and found that Helix-12 and nearby structural motifs respond dynamically in that process. Modeling showed that the agonist and antagonist/agonist form a hydrogen bond with Thr877/Asn705 and that this interaction is absent for antagonists. Agonist binding to AR increases mobility of residues at allosteric sites and co-activator binding sites, while antagonist binding decreases mobility at these important sites. A new site was also identified as a potential surface for allosteric binding. These results shed light on the effect of agonists and antagonists on the structure and dynamics of AR.

Graphical Abstract

*To whom correspondence should be addressed. Kathleen A. Durkin: durkin@berkeley.edu, Martyn T. Smith : martynts@berkeley.edu.

Supporting Information Available

Supporting information Tables S1-S12: Linear correlation coefficients for RMSF

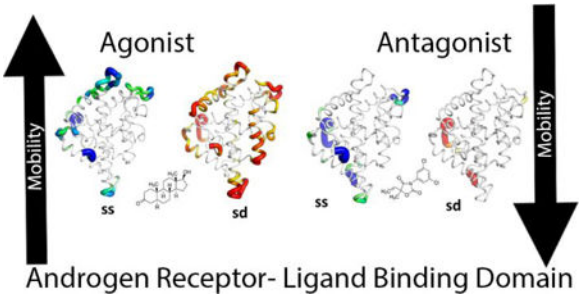

Introduction

Androgen receptor (AR) is a member of the nuclear receptor (NR) superfamily. Upon binding to endogenous androgenic ligands such as testosterone and dihydrotestosterone (DHT), AR localizes to the nucleus and binds the androgen response element to regulate the transcription of androgen sensitive genes.[1, 2] AR plays a pivotal role in regulation of many normal developmental and physiological processes including muscle hypertrophy, reproductive function, prostate and testicular development. The structure of AR consists of an N-terminal domain, DNA binding domain, and a ligand binding domain (LBD) connected by a hinge region.[3] The N-terminal and LBD control transcription via activation function 1 (AF1) and activation function 2 (AF2) sites, respectively.[3, 4] In addition to AF2, other known binding sites in the LBD include the ligand binding pocket and binding function 3 (BF3).[5] AR co-activators are proteins which bind to the AF2 site to modulate AR transcriptional action.[6]

Apart from the endogenous ligands, exogenous ligands like environmental chemicals and pharmaceuticals can also interact with AR and alter its normal function.[7] These can either act as agonists or antagonists, occupying a receptor's active site and blocking normal activation by endogenous hormones, modulating recruitment of co-activators (or co-repressors) to the transcriptional complex. Some chemicals known to cause toxicity by acting as antagonists include dicarboximide fungicides (e.g. vinclozolin and procymidone), linuron, and flutamide.[8–10]Previous studies have shown that perturbation in the AR signaling pathway is associated with many adverse health outcomes such as abnormal reproductive health, androgen insensitive syndrome, and prostate cancer.[11–13] Studies have shown that androgens and AR signaling play an important role in the development and progression of prostate cancer.[1, 2, 14–16] Pharmaceutical drugs targeting the AR signaling cascade are a primary treatment for prostate cancer. AR antagonists have been proven useful to treat prostate cancer by blocking AR activity.[17–19] Suppressing AR transcriptional activity with nonsteroidal antagonists such as hydroxyflutamide, enzalutamide and R-bicalutamide is an effective treatment for prostate cancer.[20–22] However, mutations in the ligand binding pocket of AR can alter the activity so that they instead act as agonists.[23, 24] In particular, R-bicalutamide binding to the W741L/C mutant was shown to act as an agonist.[25] In addition, Klocker and co-workers showed that bicalutamide acquires agonistic properties during long term androgen ablation.[26] Hydroxyflutamide has also been reported to exhibit agonistic effects in high concentration.[22, 27] The mechanism by which an antagonist becomes an agonist is still elusive. Claudio and co-workers have used 2.5 nanosecond (ns) molecular

dynamics simulations to understand the molecular basis of ligands as agonists or antagonists of AR.[28] However, gaining detailed knowledge about the extent and significance of the dynamics of AR when complexed to agonists as compared to antagonists requires a much greater amount of conformational sampling, because of the large number of degrees of freedom and the long-time scales involved in the collective motions of the LBD of AR. Dalton and co-workers have crystalized an AR LBD mutant form complexed with bicalutamide (PDB:1Z95),[25] providing structural insights into the agonist or antagonist effects of these ligands in AR. In general, binding of the LBD of NR to steroids is known to cause structural and dynamic changes within the LBD.[29–31] For example, binding of estrogen changes the conformation of helix 12 (H12) in the estrogen receptor.[32, 33] It is known that the overall stability of the LBD of AR increases upon binding to the native agonists. AR binding to androgens is known to affect functional regions of its LBD such as AF2 and BF3 and an unknown functional surface site.[34] Recently, Li et al, investigated the interaction between the AR agonist and antagonist and their influence on the co-activator binding using MD simulations.[34] Smieško et al utilized molecular docking and MD simulation to discriminate the agonistic and antagonist conformation of AR, showing that distinguishing AR antagonists from agonists is not possible with their current approach alone.[35] Hong et al, studied the structural changes in AR upon binding to agonist and antagonist using bicalutamide as their example antagonist, but bicalutamide is known to act as agonist in the absence of androgen and thus is not a good model.[36] Thus, the details of the local and global structural and dynamic information are missing for AR upon binding to different agonists and antagonists. Hence, in this study we address the following:

- Characterize the critical binding interactions between the AR LBD and agonist or antagonist ligands;
- Provide insight into the dynamic response of AR upon interaction with agonist and antagonist ligands using 1 microsecond long simulations and perturbation analysis;
- Identify previously unknown surface residues which can potentially induce allostery in AR.

Better understanding of conformational changes to AR upon binding to different agonist and antagonist ligands could help in rational design of novel compounds for the treatment of prostate cancer and developmental disorders. In this study, multiple one microsecond (μs) MD simulations were conducted on complexes of agonists, antagonists and antagonist/agonists bound to the AR LBD to understand the effects of these ligands on the conformation of AR.

Materials and Methods

Docking of Ligands to AR

A set of AR agonist and antagonist ligands is shown in Scheme 1. Docking of this set of ligands to LBD of AR was carried out with the Maestro software suite (Schrödinger; New York, NY, 2018–4). The agonists and antagonists were prepared for simulation using the LigPrep module.[37] Ligands were then docked to the ligand binding pocket of wild type

human AR (PDB: 3ZQT) using GLIDE docking.[38] The grid was centered on the ligand binding pocket of AR. Docking was performed using Glide's SP (Standard Precision) setting with the ligand treated flexibly.

Calculation of Partial Charges and Ligand Force Field Parameters

The agonists and antagonists of AR were subjected to optimization calculations using Gaussian 09 rev D01 and B3LYP/6–31G(d,p) level of theory.[39] and without any geometrical constraints. Partial atomic charges for the optimized geometries of the ligands were calculated using the same level of theory, using the restrained electrostatic potential (RESP) protocol based on the Gaussian generated electrostatic potential (ESP).[40] Force field parameters for the ligands were a combination of existing ones from the Generalized Amber Force Field (GAFF force field) and newly computed ones using the Antechamber module of the AMBER 18 package.[41]

Molecular Dynamics Simulation of AR/ligand complexes

MD simulations of all the docked complexes were carried out using the AMBER 18 program suite.[41] The agonist and antagonist complexes with LBD of AR obtained from the Glide docking calculations were solvated with TIP3P water.[42] Using AMBER14SB force field[43], the solvated system was subjected to 1000 steps of energy minimization employing the steepest descent and conjugate gradient algorithms. Minimization was followed by a preliminary 500 picosecond (ps) MD simulation. The 1 μs MD production run was then carried out for all systems using a 2 femtosecond (fs) time step for the integration of the equations of motion in the NPT ensemble at 300 K and at 1 atmospheric pressure. The particle-mesh Ewald (PME) method was used to calculate the long-range electrostatic interactions beyond a cutoff of 12 Å. Periodic boundary conditions were applied for all simulations with an isothermal-isobaric (NPT) ensemble at 300 K and 1 atm pressure maintained using the Langevin thermostat and Berendsen weak-coupling algorithm respectively. The collision frequency was set as 5 ps^{-1}. The SHAKE algorithm was used to constrain only hydrogen atoms.[44] The 1 μs MD production simulations for each ligand/AR complex were replicated three times, using different random seeds for the initial velocities to get good sampling of coordinate space. Post processing and analysis were carried out using GROMACS 2018.3 analysis tools.[45] VMD 1.9.4 [46] and PyMol 2.3.1[47] packages were used for visualization analysis.

Random Accelerated Molecular Dynamics Simulation (RAMD)

RAMD simulation[48] implemented in the NAMD 2.13 program suite[49] was used to investigate the potential dissociation pathways of testosterone from the ligand binding site of AR. Because the ligand could potentially exit from a variety of channels, eighty different simulations were carried out to get good statistics of the ligand exit channels. In each, a random force was applied to accelerate the ligand movement, with the force set to either 14 or 16 kcal $mol^{-1}Å^{-1}$. The initial force direction was chosen randomly by the algorithm. After each after 100 fs MD simulation the force direction was retained if the ligand center of mass moved by at least 0.025 Å. Otherwise it was randomly changed. Simulations were terminated when the center of mass of the ligand had moved further than 30 Å from its

original position. The exit event occurs at different time scale for each simulation, but the maximum length of the simulation is set to 3 ns. Coordinates were saved at 1 ps intervals.

Perturbation–response Decomposition of Molecular Dynamics Trajectories

A covariance matrix $\left(Q = RT\sum_{n=1}^{3N} |n\rangle\lambda_n\langle n|\right)$ was constructed for each MD trajectory using the JED package.[50] The effective Hessian matrix is obtained from $H_o = RT\ Q^{-1}$. The random noise was removed by substitution $\lambda_n \rightarrow \langle\lambda\rangle_{n \geq c} = \frac{1}{3N-c}\sum_{n=c}^{3N}\lambda_n$ over the $n \geq c$ subspace as explained in our previous methods paper.[51] Perturbation was applied to the effective Hessian matrix with spring constant of 10 kcal/mol/Å^2 within radius of 10 Å. The perturbation response profile was calculated using the method previously described.[51] The response and perturbation profiles were further decomposed into perturbation which gives rise to stabilizing response (decrease in mobility) and destabilizing response (increase in mobility) as described in our previous study.

Results and Discussion

Differences in the Interaction of Agonist and Antagonist Ligands with AR

Agonist and antagonist ligands were docked into the ligand binding pocket of AR. The predicted binding modes of all the ligands are shown in Figure 1, revealing that all agonists form a hydrogen bond (H-bond) with Arg752. 17β-trenbolone and testosterone have an additional H-bond with Asn705, whereas methyltrienolone, a synthetic androgen forms an H-bond with Thr877. Neburon has an H-bond interaction with Leu-704 while the other antagonists lack H-bonds donor or acceptor. Bicalutamide and hydroxyflutamide, which can either act as agonists or antagonists, forms H-bonds with Asn705 and Arg752. The main difference between the agonist and antagonist ligand binding is the presence or absence of these H-bonds between the ligand and the receptor.

Structure and Dynamics of AR upon Binding to Ligands

To explore the structure and dynamics of the binding modes of different ligands in the AR LBD, we conducted MD-based simulations of docked AR-ligand complexes as described in Materials and Methods. To evaluate the conformational dynamics induced by different agonists and antagonists, the root mean square fluctuation (RMSF) for each residue was calculated for the last 500 ns simulation and averaged over the three simulations. Figure 2 displays the variation of RMSF of each residue of the AR LBD with the individual ligands. Linear correlation coefficients for RMSF between all the ligand-AR complexes are given in Table S1. The tabulated data indicate that there is overall similarity in RMSF between all the complexes. Linear correlation coefficients for RMSF between different Helix and loops are given in the supporting information Table S2–S12. The correlation values indicate that the RMSF profile varies most strongly in H3, the loop between H3 and H4, H12 and the loop between H11 and H12. H6 of Bicalutamide-AR complex deviates the most from all other AR complexes. These observations highlight that the primary dynamics of AR-agonist, AR-antagonist and AR-agonist/antagonist complexes differ mainly at H3, H12 and the nearby loops.

Hydrogen Bonds between Ligands and AR

Docking results show that H-bonds between ligands and AR play an important role in their binding. The residues involving in the formation of H-bonds with different ligands with their occupancies are given in the Table 1.

A striking difference between the agonist and antagonist binding modes is the absence of H-bonding interaction between the AR and antagonist ligands. Potent agonists such as DHT, 17β-trenbolone, and methyltrienolone all form an H-bond with Thr877 with a time averaged occupancy of more than 90%, whereas testosterone forms an H-bond with Asn705 but also with high occupancy. In contrast, neither Thr877 nor Asn705 have H-bonding interactions with the known antagonists. Both hydroxyflutamide and bicalutamide have an H-bond with Asn705 with occupancy of 21.70 and 46.70% respectively. Both hydroxyflutamide and bicalutamide form an H-bond with Leu704 with higher occupancy of 62.10% and 90.83 respectively.

Binding-Free Energy Analysis using MM-PBSA

To gain further insight into the binding affinity between the various ligands and AR, ΔG_{bind} was calculated using the standard MM-PBSA method implemented in AMBER 18.[41] The calculated binding free energies were averaged over the last 50 ns from three different imulations performed with each ligand/AR complex. The results are given in in Table 2 and indicate that the binding free energies of agonists are in the range ~−14 to ~−16 kcal/mol, whereas the values for the antagonist and agonist/antagonist are slightly weaker with the values ranging from −8 to −12 kcal/mol. By molecular mechanics (MM) calculation in gas phase, the van der Waals interactions (ΔE_{vdW}) contributions were similar in all the systems, whereas stronger electrostatic (ΔE_{ele}) interactions were observed in all agonist and agonist/antagonist complexes. For agonist/antagonist complexes it is the stronger electrostatic interaction which contributes significantly to the overall binding free energies.

Change in Dynamic Response

To understand the change in the AR dynamics/mobility upon binding to different ligands, we followed a previously published methodology to compute and decompose the responses to the perturbation.[51] The average dynamic response profile is decomposed into stabilizing response (ss) and destabilizing response (sd). The relative degrees of change in the response to the stabilizing perturbation for agonist, antagonist and agonist/antagonist complex are summarized in Table 3. $\langle|\Delta TR|\rangle$ is average change in trace of covariance matrix upon stabilizing perturbation, which explains the overall magnitude of the dynamic response. Binding of an antagonist decreases the dynamic response of the AR when compared to the apo AR, whereas binding of an agonist either slightly increases or decreases the dynamic response, depending on the specific ligand molecule. A two-fold increase in the dynamic response has been observed for the bicalutamide-AR complex. The $\langle|\Delta TR|\rangle$ data are normalized relative to the apo so that each protein is assigned a relative percent (*rel%S*) of dynamic response for stabilizing perturbations. The relative percentage is decomposed into relative percentage of stabilizing perturbation leading to stabilizing response (*%ss*) and relative percentage of stabilizing perturbation leading to destabilizing response (*%sd*). It can be seen from the table that overall characteristics of dynamic response for the agonist and

agonist/antagonist is similar, while for the antagonist the relative percentage of stabilizing response increases, and the relative percentage of destabilizing response decreases with respect to the apo AR.

The mean response profile (ss and sd) mapped on to the structures of AR is shown in Figure 3. The mean response profiles are similar for the apo AR, the agonist and agonist/antagonist AR complexes. Similar trends in agonist complexes show the strong sd in Helix-7, Helix-12, and in the allosteric sites BF3 and AF2 sites[52] (Figure 3b to 3e). In antagonist complexes, the Helix 12 and AF2 display strong ss. Previous studies show that protein regions with high flexibility/mobility play important roles in favorable binding with binding partners and in allosteric regulation.[53–55] Taken together, the results suggest that all agonists increase mobility in the AF2 and BF3 regions which will then enable binding to coactivators.[56] Hydroxyflutamide and bicalutamide trigger similar responses to that of agonists. These ligands can act as agonists at high concentration or in the absence of androgens.[22, 26, 27] The agonism/antagonism of these ligands is determined by the affinity to bind at the ligand binding pocket by replacing the natural androgens.

Dissociation of Androgen from the AR Ligand Binding Pocket

The ligand binding pocket of AR is buried deep inside the LBD. It is important to comprehend the mechanism of the ligand entry/exit to this deep pocket to understand which residues and structural motifs respond dynamically in that process. Hence, testosterone was docked in the ligand binding site of AR and fifty steps of RAMD simulations were carried out as described in the methods section. RAMD simulation was originally designed to give ideas about egress routes from buried ligand binding sites and therefore hint at ligand access routes.[57] Wade and co-workers have proposed the ligand access and exit route based on the RAMD simulations for P450.[5758]The RAMD trajectories revealed the unbinding of testosterone through three different channels A, B and C (Figure 4a). 62.50% of egress trajectories were via channel A, another 26.25% via channel B, and the rest 11.25% via channel C. Residues involved in each channel are given in Table 4. Channel A is created by the loop between Helix 11 and Helix 12 (Figure 4b). From the previous studies it is well known that in nuclear receptors in general, Helix 12 is more flexible in the apo AR form and that ligand binding stabilizes the ligand binding domain.[30] Even though the ligand entry and exit pathway from the buried pocket could vary, in this study we assume that exit channel is also the substrate entry channel. Thus, we propose that the channel A is the most probable entry/exit route for ligands in AR. Channel B (Figure 4c) is located in between the Helix 1 and Helix 4 as shown in Figure 4c. In channel C (Figure 4d), the ligand exits by the channel created by AF2. The recruitment of a co-activator at the AF2 region of channel C may stabilize the overall structure of AR and prevent the exit of agonist ligands from the pocket through this channel.

Identification of Possible Allosteric Sites

The AR surface has allosteric ligand binding sites that modulate AR activity.[52]. So far, three such sites have been identified in AR, namely AF2, BF3 and BF4.[52] Targeting these surface sites has yielded new therapeutics for prostate cancer.[52] We used the default settings of the SiteMap site recognition software in the Maestro Schrödinger[59, 60] suite to identify potential

AR ligand-binding surface sites. SiteMap predicted three surface sites as shown in Figure 5a. The volume and SiteScore data are given in Table 5. Site 1 has a SiteScore of 0.898 and is predicted to be a possible binding surface site. Further, our perturbation studies show that the residues in Site 1 and Site 2 can trigger stabilizing and destabilizing responses respectively. The mean perturbation profile for the apo AR is depicted in the Figure 5b. It can be seen from the figure that the residues in the allosteric site (BF3) trigger the stabilizing response, which rigidifies the ligand binding domain. Also, the Site 1 surface formed by the residues from Helix-7 and Helix-10/11 is shown to trigger a stabilizing response similar to that of known allosteric site BF3. Taking this data together, we propose that Site 1 surface formed by the Helix-7 and Helix-10/11 may be a previously unidentified allosteric site. When a moiety binds to this Site 1 surface, it may rigidify and restrict the entry of the natural ligand.

Taken together, we speculate that the increase in mobility of the residues in the AF2 and BF3 sites upon agonist binding in the LBP helps in binding the co-activators which in-turn transfer allosteric signal to the DNA binding domain for its transcriptional activity. Other studies have also shown that nuclear receptor coactivators enhance AR-mediated transactivation[61, 62]

Conclusion

We describe here long-time scale conformational fluctuations in the AR LBD structure when bound to agonists and antagonists. We identify the channel near Helix-12 as the most probable entry/exit route for ligands in the AR ligand binding pocket. Agonists and antagonists exhibit distinct binding modes, with agonists forming an H-bond with either Thr877 or Asn705. Generally, agonists transfer an allosteric signal through Helix-7 to the cofactor binding pocket by increasing the mobility of Helix-7, Helix-12, AF2 and BF3, while antagonists increase the overall stability of the LBD of AR. The flexibility induced by agonists enables coactivator binding and stabilizes the complex. Hydroxyflutamide and bicalutamide show a similar dynamic response to that of agonist with the slightly weaker H-bond with Thr877 or Asn705. Agonistic activity of these ligands is determined by the binding affinity and the ability to replace the endogenous androgens. We also identified another previously unknown surface site on the AR LBD which may bind small molecules and alter the normal function of AR.

Supplementary Material

Refer to Web version on PubMed Central for supplementary material.

Acknowledgements:

This project was supported by contracts 17-E0023 (to MTS) and 17-E0024 (to MAL) from the Office of Environmental Health Hazard Assessment of the California Environmental Protection Agency.

Reference

1. Davey RA; Grossmann M Androgen receptor structure, function and biology: from bench to bedside. Clin. Biochem. Rev 2016, 37, 3–15. [PubMed: 27057074]

2. Shafi AA; Yen AE; Weigel NL Androgen receptors in hormone-dependent and castration-resistant prostate cancer. Pharmacol. Ther 2013, 140, 223–238. [PubMed: 23859952]

3. Gao W; Bohl CE; Dalton JT Chemistry and structural biology of androgen receptor. Chem. Rev 2005, 105, 3352–3370. [PubMed: 16159155]

4. Jenster G; van der Korput HA; van Vroonhoven C; van der Kwast TH; Trapman J; Brinkmann AO Domains of the human androgen receptor involved in steroid binding, transcriptional activation, and subcellular localization. Mol. Endocrinol 1991, 5, 1396–1404. [PubMed: 1775129]

5. Estebanez-Perpina E; Arnold LA; Nguyen P; Rodrigues ED; Mar E; Bateman R; Pallai P; Shokat KM; Baxter JD; Guy RK; et al. A surface on the androgen receptor that allosterically regulates coactivator binding. Proc. Natl. Acad. Sci. U.S.A 2007, 104, 16074–16079. [PubMed: 17911242]

6. Askew EB; Gampe RT Jr.; Stanley TB; Faggart JL; Wilson EM Modulation of androgen receptor activation function 2 by testosterone and dihydrotestosterone. J. Biol. Chem 2007, 282, 25801–25816. [PubMed: 17591767]

7. Delfosse V; Maire AL; Balaguer P; Bourguet W A Structural perspective on nuclear receptors as targets of environmental compounds. Acta. Pharmacol. Sin 2015, 36, 88–101. [PubMed: 25500867]

8. Martinovic D; Blake LS; Durhan EJ; Greene KJ; Kahl MD; Jensen KM; Makynen EA; Villeneuve DL; Ankley GT Reproductive toxicity of vinclozolin in the fathead minnow: confirming an anti-androgenic mode of action. Environ. Toxicol. Chem 2008, 27, 478–488. [PubMed: 18348629]

9. Lambright C; Ostby J; Bobseine K; Wilson V; Hotchkiss AK; Mann PC; Gray LE Jr. Cellular and molecular mechanisms of action of linuron: an antiandrogenic herbicide that produces reproductive malformations in male rats. Toxicol. Sci 2000, 56, 389–399. [PubMed: 10910998]

10. Zacharia LC Permitted daily exposure of the androgen receptor antagonist flutamide. Toxicol. Sci 2017, 159, 279–289. [PubMed: 28666357]

11. Shtivelman E; Beer TM; Evans CP Molecular pathways and targets in prostate cancer. Oncotarget 2014, 5, 7217–7259. [PubMed: 25277175]

12. Matsumoto T; Sakari M; Okada M; Yokoyama A; Takahashi S; Kouzmenko A; Kato S The androgen receptor in health and disease. Annu. Rev. Physiol 2013, 75, 201–224. [PubMed: 23157556]

13. Lonergan PE; Tindall DJ Androgen receptor signaling in prostate cancer development and progression. J. Carcinog 2011, 10, 20–34. [PubMed: 21886458]

14. Banerjee PP; Banerjee S; Brown TR; Zirkin BR Androgen action in prostate function and disease. Am. J. Clin. Exp. Urol 2018, 6, 62–77. [PubMed: 29666834]

15. Fujita K; Nonomura N Role of androgen receptor in prostate cancer: A Review. World. J. Mens. Health 2018, 36, 1–8. [PubMed: 29299901]

16. Newschaffer CJ; Otani K; McDonald MK; Penberthy LT Causes of death in elderly prostate cancer patients and in a comparison nonprostate cancer cohort. J. Natl. Cancer. Inst 2000, 92, 613–621. [PubMed: 10772678]

17. Wadosky KM; Koochekpour S Therapeutic rationales, progresses, failures, and future directions for advanced prostate cancer. Int. J. Biol. Sci 2016, 12, 409–426. [PubMed: 27019626]

18. Munoz J; Wheler JJ; Kurzrock R Androgen receptors beyond prostate cancer: an old marker as a new target. Oncotarget 2015, 6, 592–603. [PubMed: 25595907]

19. Masiello D; Cheng S; Bubley GJ; Lu ML; Balk SP Bicalutamide functions as an androgen receptor antagonist by assembly of a transcriptionally inactive receptor. J. Biol. Chem 2002, 277, 26321–26326. [PubMed: 12015321]

20. Goldspiel BR; Kohler DR Flutamide: an antiandrogen for advanced prostate cancer. DICP 1990, 24, 616–623. [PubMed: 2193461]

21. Culig Z Molecular mechanisms of enzalutamide resistance in prostate cancer. Curr. Mol. Biol. Rep 2017, 3, 230–235. [PubMed: 29214142]

22. Kemppainen JA; Wilson EM Agonist and antagonist activities of hydroxyflutamide and casodex relate to androgen receptor stabilization. Urology 1996, 48, 157–163. [PubMed: 8693644]

23. Hara T; Miyazaki J; Araki H; Yamaoka M; Kanzaki N; Kusaka M; Miyamoto M Novel mutations of androgen receptor: a possible mechanism of bicalutamide withdrawal syndrome. Cancer. Res 2003, 63, 149–153. [PubMed: 12517791]

24. Taplin ME; Bubley GJ; Shuster TD; Frantz ME; Spooner AE; Ogata GK; Keer HN; Balk SP Mutation of the androgen-receptor gene in metastatic androgen-independent prostate cancer. N. Engl. J. Med 1995, 332, 1393–1398. [PubMed: 7723794]
25. Bohl CE; Gao W; Miller DD; Bell CE; Dalton JT Structural basis for antagonism and resistance of bicalutamide in prostate cancer. Proc. Natl. Acad. Sci. U.S.A 2005, 102, 6201–6206. [PubMed: 15833816]
26. Culig Z; Hoffmann J; Erdel M; Eder IE; Hobisch A; Hittmair A; Bartsch G; Utermann G; Schneider MR; Parczyk K; Klocker H Switch from antagonist to agonist of the androgen receptor bicalutamide is associated with prostate tumour progression in a new model system. Br. J. Cancer 1999, 81, 242–251. [PubMed: 10496349]
27. Wilding G; Chen M; Gelmann EP Aberrant response in vitro of hormone-responsive prostate cancer cells to antiandrogens. Prostate 1989, 14, 103–115. [PubMed: 2710689]
28. Bisson WH; Abagyan R; Cavasotto CN Molecular basis of agonicity and antagonicity in the androgen receptor studied by molecular dynamics simulations. J. Mol. Graph. Model 2008, 27, 452–458. [PubMed: 18805032]
29. Sever R; Glass CK Signaling by nuclear receptors. Cold Spring Harb. Perspect. Biol 2013, 5, a016709–a016709. [PubMed: 23457262]
30. Huang P; Chandra V; Rastinejad F Structural overview of the nuclear receptor superfamily: insights into physiology and therapeutics. Annu. Rev. Physiol 2010, 72, 247–272. [PubMed: 20148675]
31. Jin L; Li Y Structural and functional insights into nuclear receptor signaling. Adv. Drug. Deliv. Rev 2010, 62, 1218–1226. [PubMed: 20723571]
32. Shiau AK; Barstad D; Loria PM; Cheng L; Kushner PJ; Agard DA; Greene GL The structural basis of estrogen receptor/coactivator recognition and the antagonism of this interaction by tamoxifen. Cell 1998, 95, 927–937. [PubMed: 9875847]
33. Ho BK; Agard DA Probing the flexibility of large conformational changes in protein structures through local perturbations. PLoS. Comput. Biol 2009, 5, e1000343–e1000356. [PubMed: 19343225]
34. Jin Y; Duan M; Wang X; Kong X; Zhou W; Sun H; Liu H; Li D; Yu H; Li Y; Hou T Communication between the ligand-binding pocket and the activation function-2 domain of androgen receptor revealed by molecular dynamics simulations. J. Chem. Inf. Model 2019, 59, 842–857. [PubMed: 30658039]
35. Wahl J; Smiesko M Endocrine disruption at the androgen receptor: employing molecular dynamics and docking for improved virtual screening and toxicity prediction. Int. J. Mol. Sci 2018, 19, 7184–7200.
36. Sakkiah S; Kusko R; Pan B; Guo W; Ge W; Tong W; Hong H Structural changes due to antagonist binding in ligand binding pocket of androgen receptor elucidated through molecular dynamics simulations. Front. Pharmacol 2018, 9, 492–505. [PubMed: 29867496]
37. LigPrep, Schrödinger release 2019–2: Schrödinger, LLC, New York, NY, 2019.
38. Friesner RA; Banks JL; Murphy RB; Halgren TA; Klicic JJ; Mainz DT; Repasky MP; Knoll EH; Shelley M; Perry JK; et al. Glide: a new approach for rapid, accurate docking and scoring. 1. method and assessment of docking accuracy. J. Med. Chem 2004, 47, 1739–1749. [PubMed: 15027865]
39. Frisch MJ; Trucks GW; Schlegel HB; Scuseria GE; Robb MA; Cheeseman JR; Scalmani G; Barone V; Mennucci B; Petersson GA, et al. Gaussian 09, Revision A.1; Gaussian, Inc: Wallingford,CT, 2009.
40. Bayly CI; Cieplak P; Cornell WD; Kollman PA A well-behaved electrostatic potential based method using charge restraints for deriving atomic charges - the resp model. J. Phys. Chem 1993, 97, 10269–10280.
41. Case D; Ben-Shalom I; Brozell S; Cerutti D; Cheatham T III; Cruzeiro V; Darden T; Duke R; Ghoreishi D; Gilson M, et al. Amber 2018: San Francisco. California: 2018.
42. Jorgensen WL; Chandrasekhar J; Madura JD; Impey RW; Klein ML Comparison of simple potential functions for simulating liquid water. J. Chem. Phys 1983, 79, 926–935.

43. Maier JA; Martinez C; Kasavajhala K; Wickstrom L; Hauser KE; Simmerling C FF14SB: improving the accuracy of protein side chain and backbone parameters from FF99sb. J. Chem. Theory. Comput 2015, 11, 3696–3713. [PubMed: 26574453]
44. Ryckaert J-P; Ciccotti G; Berendsen HJ Numerical integration of the cartesian equations of motion of a system with constraints: molecular dynamics of n-alkanes. J. Comput. Phys 1977, 23, 327–341.
45. Van Der Spoel D; Lindahl E; Hess B; Groenhof G; Mark AE; Berendsen HJ Gromacs: fast, flexible, and free. J. Comput. Chem 2005, 26, 1701–1718. [PubMed: 16211538]
46. Humphrey W; Dalke A; Schulten K, VMD: visual molecular dynamics. J. Mol. Graph 1996, 14, 33–38. [PubMed: 8744570]
47. The PyMOL Molecular Graphics System, Schrodinger, LLC, Version 2.3.1. 2015.
48. Kokh DB; Amaral M; Bomke J; Gradler U; Musil D; Buchstaller HP; Dreyer MK; Frech M; Lowinski M; Vallee F; et al. Estimation of drug-target residence times by tau-random acceleration molecular dynamics simulations. J. Chem. Theory. Comput 2018, 14, 3859–3869. [PubMed: 29768913]
49. Phillips JC; Braun R; Wang W; Gumbart J; Tajkhorshid E; Villa E; Chipot C; Skeel RD; Kale L; Schulten K Scalable molecular dynamics with NAMD. J. Comput. Chem 2005, 26, 1781–1802. [PubMed: 16222654]
50. David CC; Singam ERA; Jacobs DJ JED: a java essential dynamics program for comparative analysis of protein trajectories. BMC Bioinform 2017, 18, 271–280.
51. Ettayapuram Ramaprasad AS; Uddin S; Casas-Finet J; Jacobs DJ decomposing dynamical couplings in mutated scfv antibody fragments into stabilizing and destabilizing effects. J. Am. Chem. Soc 2017, 139, 17508–17517. [PubMed: 29139290]
52. Grosdidier S; Carbo LR; Buzon V; Brooke G; Nguyen P; Baxter JD; Bevan C; Webb P; Estebanez-Perpina E; Fernandez-Recio J Allosteric conversation in the androgen receptor ligand-binding domain surfaces. Mol. Endocrinol 2012, 26, 1078–1090. [PubMed: 22653923]
53. Amaral M; Kokh DB; Bomke J; Wegener A; Buchstaller HP; Eggenweiler HM; Matias P; Sirrenberg C; Wade RC; Frech M Protein conformational flexibility modulates kinetics and thermodynamics of drug binding. Nat. Commun 2017, 8, 2258–2276. [PubMed: 29273720]
54. Gunasekaran K; Ma B; Nussinov R Is allostery an intrinsic property of all dynamic proteins? Proteins 2004, 57, 433–443. [PubMed: 15382234]
55. Luque I; Freire E Structural stability of binding sites: consequences for binding affinity and allosteric effects. Proteins 2000, 4, 63–71. [PubMed: 11013401]
56. Jasuja R; Ulloor J; Yengo CM; Choong K; Istomin AY; Livesay DR; Jacobs DJ; Swerdloff RS; Miksovska J; Larsen RW; Bhasin S Kinetic and thermodynamic characterization of dihydrotestosterone-induced conformational perturbations in androgen receptor ligand-binding domain. Mol. Endocrinol 2009, 23, 1231–1241. [PubMed: 19443608]
57. Ludemann SK; Lounnas V; Wade RC How do substrates enter and products exit the buried active site of cytochrome P450cam? 1. Random expulsion molecular dynamics investigation of ligand access channels and mechanisms. J. Mol. Biol 2000, 303, 797–811. [PubMed: 11061976]
58. Winn PJ; Ludemann SK; Gauges R; Lounnas V; Wade RC Comparison of the dynamics of substrate access channels in three cytochrome P450s reveals different opening mechanisms and a novel functional role for a buried arginine. Proc. Natl. Acad. Sci. U.S.A 2002, 99, 5361–5366. [PubMed: 11959989]
59. Halgren TA Identifying and characterizing binding sites and assessing druggability. J. Chem. Inf. Model 2009, 49, 377–389. [PubMed: 19434839]
60. Halgren T New method for fast and accurate binding-site identification and analysis. Chem. Biol. Drug. Des 2007, 69, 146–148. [PubMed: 17381729]
61. Voegel JJ; Heine MJ; Zechel C; Chambon P; Gronemeyer H TIF2, a 160 kDa transcriptional mediator for the ligand-dependent activation function AF-2 of nuclear receptors. EMBO. J 1996, 15, 3667–3675. [PubMed: 8670870]
62. Yeh S; Chang C Cloning and characterization of a specific coactivator, ARA70, for the androgen receptor in human prostate cells. Proc. Natl. Acad. Sci. U.S.A 1996, 93, 5517–5521. [PubMed: 8643607]

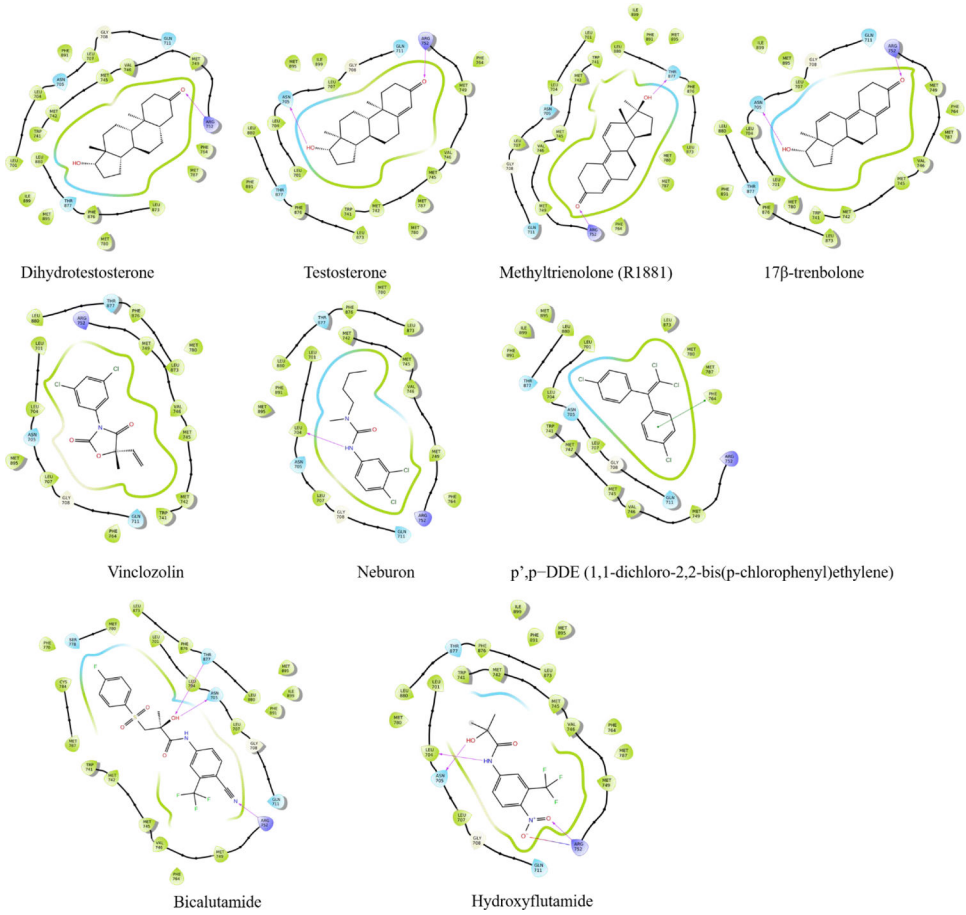

Figure 1:
Two-dimensional schematic representations of AR and different ligand interactions, (Top) agonists, (middle) antagonists, (bottom) agonist/antagonists.

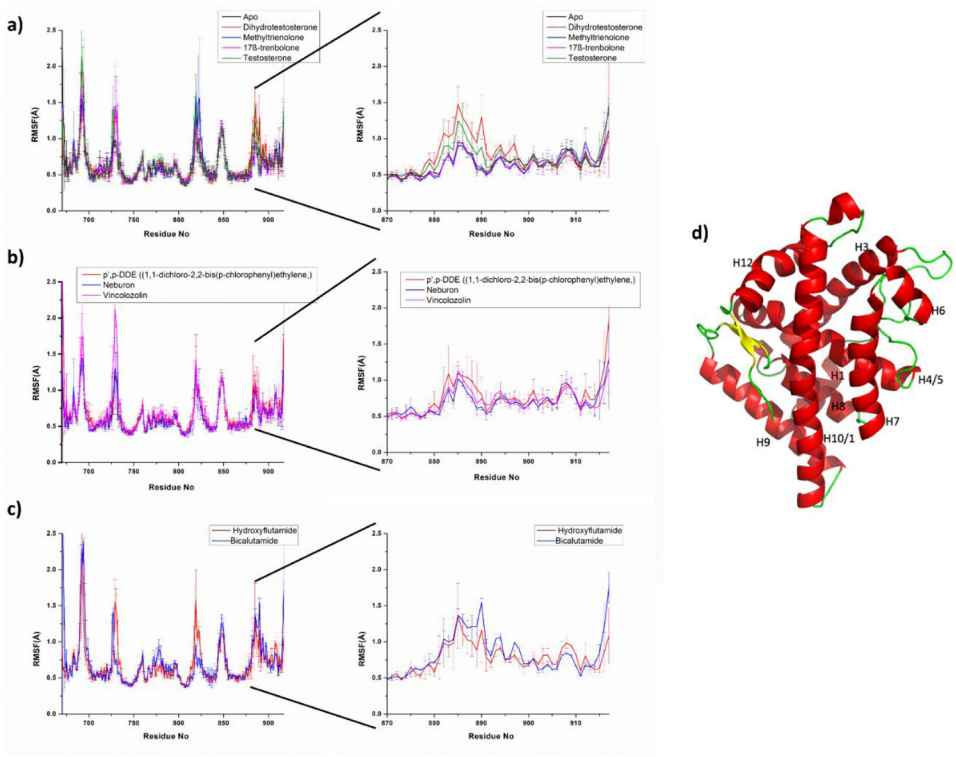

Figure 2:

Average Residue-based RMSF relative to the initial structure for each system during the last 500 ns MD trajectories for (a) AR-Agonist, (b) AR-Antagonist, (c) AR-Agonist/Antagonist, and (d) Cartoon representation of AR-LBD with the helices labeled. Arrow showing the region where the RMSF is different between different ligands.

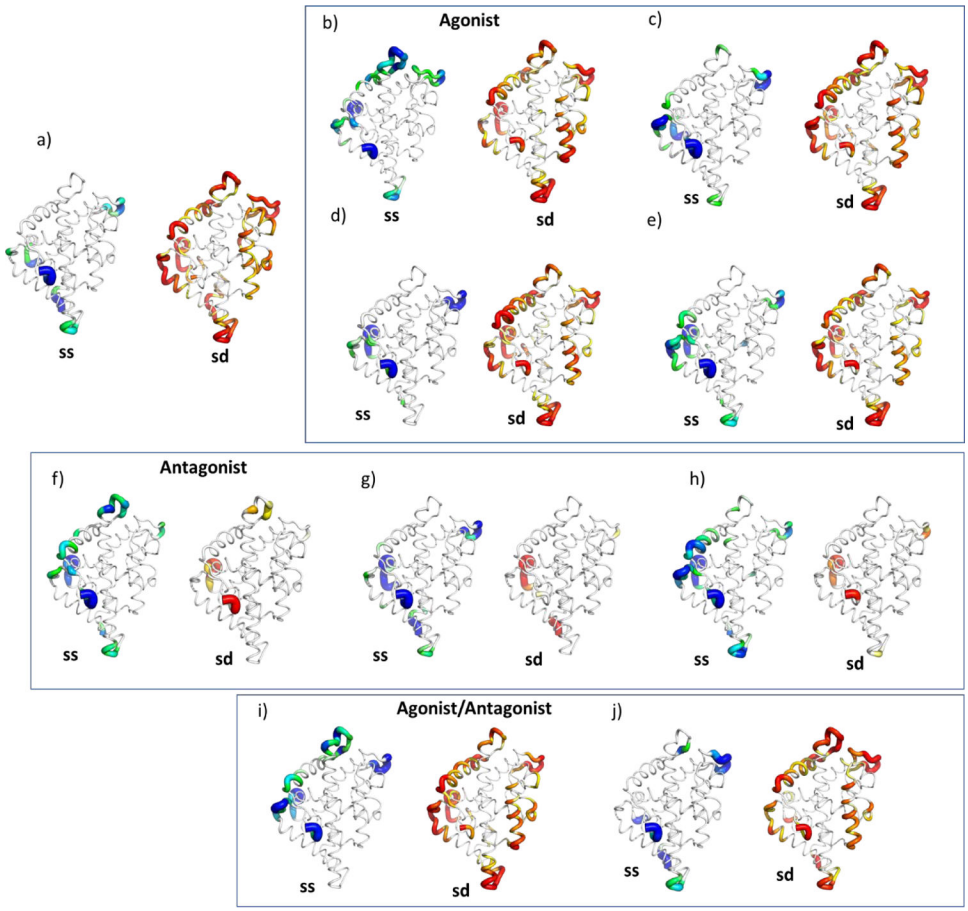

Figure 3.

Mean response profiles (ss and sd cases) mapped onto structure for (a) Apo AR, (b) DHT, (c) Testosterone, (d) 17β-trenbolone, (e) Methyltrienolone, (f) p',p−DDE (1,1-dichloro-2,2-bis(p-chlorophenyl)ethylene), (g) Vinclozolin, (h) Neburon, (i) Hydroxyflutamide and (j) Bicalutamide. The destabilizing response color scheme is from red, orange, and yellow orders destabilizing response from largest to smallest. For stabilizing response, the color scheme is set to blue, cyan, and green orders from largest to smallest. white color signifies no response.

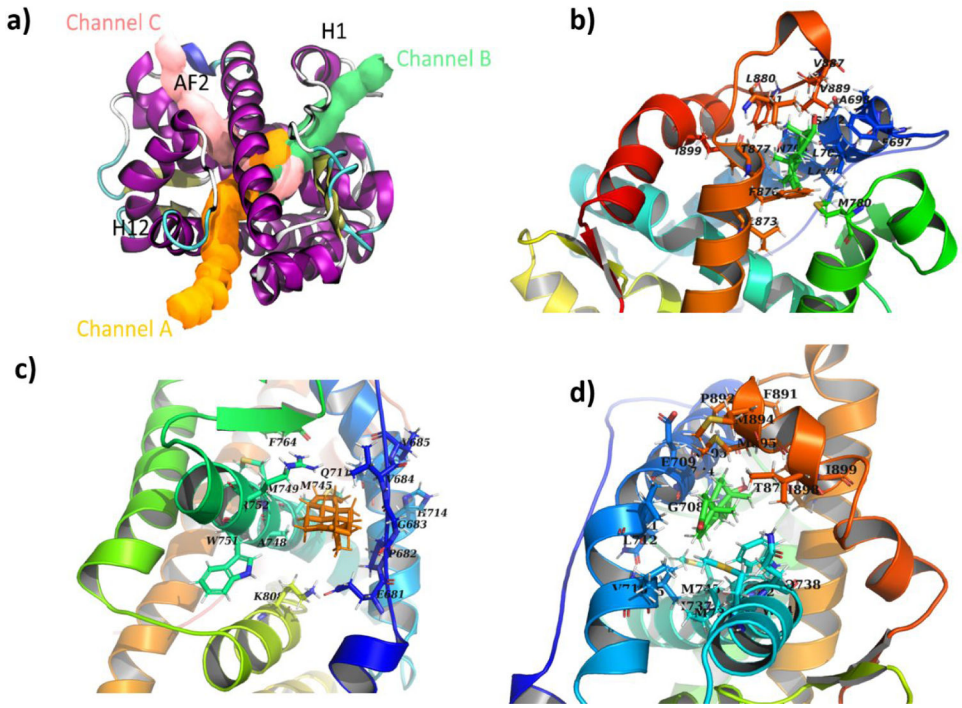

Figure 4.

a) Ligand exiting Channels, Snapshot showing the interaction between the ligand and the protein b) Channel-A, c) Channel-B, d) Channel-C

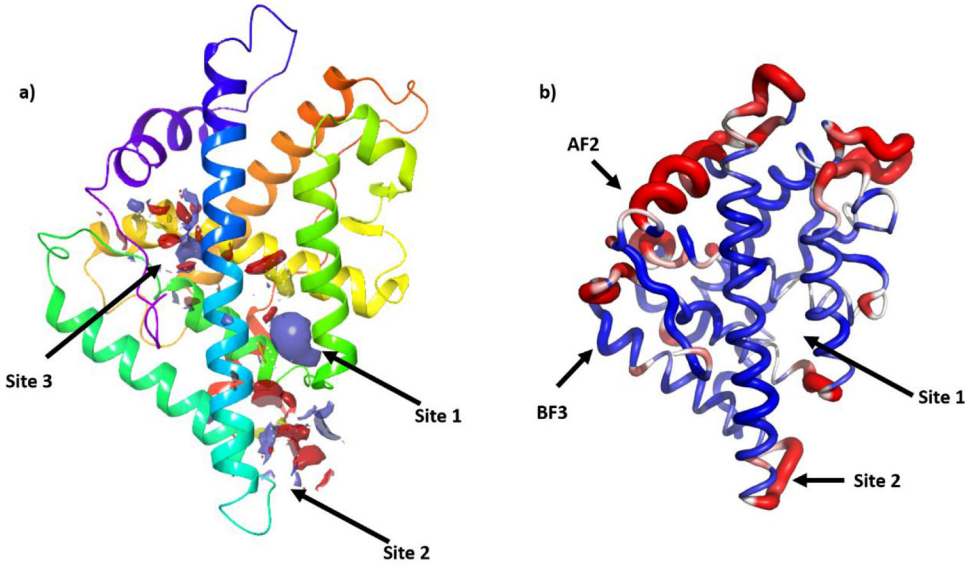

Figure 5.

a) Stabilizing perturbation profiles mapped on to the structure of LBD of AR (PDB: 3ZQT). Colored based on the residues triggering stabilizing (blue) and destabilizing (red) response. White color indicates no response. b) Predicted surface pockets identified by SiteMap

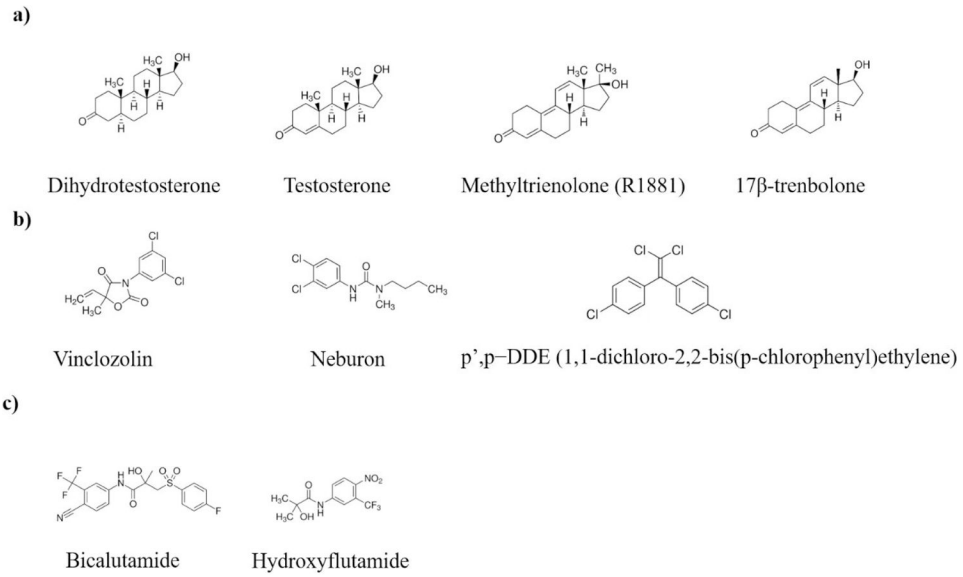

Scheme 1:

List of a) agonist and b) antagonist and c) agonist/antagonist ligands studied in this investigation.

Table 1:

Hydrogen bonds between the LBD and different ligands with their occupancy

Agonist	Residue no.	Ligand	Occupancy (%)
	Thr877	DHT	93.80±9.01
	Asn705	Testosterone	98.60±0.53
	Thr877	17β-trenbolone	98.20±0.10
	Thr877	Methyltrienolone (R1881)	98.90±0.10
	Arg752	Methyltrienolone (R1881)	10.45±5.87
Antagonist			
	-	Vinclozolin	-
	Leu704	Neburon	17.90±12.60
	-	p',p-DDE (1,1-dichloro-2,2-bis(p-chlorophenyl)ethylene)	-
Agonist / Antagonist			
	Asn705	Hydroxyflutamide	62.10±30.97
	Leu704	Hydroxyflutamide	21.70±10.87
	Thr877	Hydroxyflutamide	37.85±33.44
	Leu704	Bicalutamide	90.83±8.45
	Asn705	Bicalutamide	46.70±3.18

Table 2:

MM-PBSA binding free energies and their energy components for all of the ligand-AR complexes.

System	ΔE_{vdW} (kcal/mol)	ΔE_{elec} (kcal/mol)	ΔG_{PB} (kcal/mol)	ΔG_{SASA} (kcal/mol)	$-T\Delta S$ (kcal/mol)	ΔG_{bind} (kcal/mol)
Dihydrotestosterone	−48.04±2.28	−10.84±2.41	−57.78±3.02	19.23±2.35	−20.49±3.32	−18.06±4.40
Testosterone	−46.91±2.18	−25.77±2.34	−72.69±2.76	35.82±1.88	−20.40±2.55	−16.46±3.84
17β-trenbolone	−43.77±2.35	−22.31±2.80	−66.08±2.98	30.52±3.53	−20.55±3.04	−15.01±4.46
Methyltrienolone	−46.00±2.31	−23.70±3.31	−69.70±3.37	31.07±2.62	−21.90±3.13	−16.74±4.24
p',p−DDE (1,1-dichloro-2,2-bis(p-chlorophenyl)ethylene)	−41.90±1.84	−1.32±0.80	−43.22±1.96	12.58±1.74	−18.46±2.81	−12.18±3.75
Vinclozolin	−41.43±2.00	2.65±1.50	−38.78±2.37	11.37±1.37	−21.31±2.84	−8.22±3.91
Neburon	−44.74±2.07	−16.77±1.90	−61.52±2.92	29.21±2.48	−20.35±3.02	−11.95±3.79
Hydroxyflutamide	−40.10±2.35	−31.41±3.74	−71.51±3.85	42.74±3.32	−20.47±3.29	−8.29±4.70
Bicalutamide	−54.64±2.64	−33.93±4.25	−88.57±4.61	52.28±4.38	−23.63±3.99	−12.66±5.30

Table 3:

Relative distribution characteristics of dynamic response to stabilizing perturbations for all of the ligand-AR complexes.

System	$\langle\lvert\Delta TR\rvert\rangle$	*rel%S*	*%ss*	*%sd*
Apo	4.01	100.00	68.45	31.55
17β-trenbolone	6.42	160.40	70.67	29.33
DHT	3.09	77.22	74.27	25.73
Methyltrienolone	4.16	103.92	73.56	26.44
Testosterone	4.48	111.78	71.41	28.59
p',p−DDE (1,1-dichloro-2,2-bis(p-chlorophenyl)ethylene)	1.15	28.77	91.15	8.85
Neburon	0.61	15.22	93.49	6.51
Vinclozolin	1.78	44.35	91.81	8.19
Hydroxyflutamide	5.61	140.00	70.38	29.62
Bicalutamide	10.79	269.47	71.24	28.77

Table 4:

Amino acid residues in the different channels for ligand unbinding

Channels	Residues involved
Channel A	I899, L873, T877, L880, F896, M780, V887, A698, F697, V889, L701, S702, L704, N705, F891
Channel B	F764, V684, V685, R752, M749, W751, A748, M745, M683, Q711, P682, H714, E681, K808
Channel C	L704, N705, E709, G709, Q711, L712, V715, V716, M734, I737, Q738, W741, M742, M745, T877, F891, P892, M895, I899

Table 5:

Different sites predicted from the Sitemap with score and volume

Sites	Volume (Å^3)	SiteScore
Site 1	108.045	0.898
Site 2	93.296	0.710
Site 3	93.296	0.709